Physica A 556 (2020) 124851

Contents lists available at ScienceDirect

Physica A

journal homepage: www.elsevier.com/locate/physa

The $R_{q,Q}$ function and the q-Diode

R.V. Ramos

Lab. of Quantum Information Technology, Department of Teleinformatic Engineering, Federal University of Ceara - DETI/UFC, C.P. 6007, Campus do Pici, 60455-970 Fortaleza-Ce, Brazil

ARTICLE INFO

Article history:
Received 19 February 2020
Received in revised form 19 May 2020
Available online 23 June 2020

Keywords:
Lambert–Tsallis W_q function
q-exponential
Disentropy
Diode

ABSTRACT

Two generalizations of the Lambert W function were recently discussed in the literature, the Lambert–Tsallis W_q and the Lambert–Kaniadakis W_κ functions. Both of them have been used in interesting problems in physics and engineering. In this direction, the present work introduces a third generalization, the new function $R_{q,Q}(z)$, solution of the equation $R_{q,Q}(z) \times_Q \exp_q(R_{q,Q}(z)) = z$. It is shown this new function can be used to construct new disentropy as well it is used to model the q-diode, a hypothetical electronic device whose electrical current depends q-exponentially on the voltage between its terminals. Analytical and numerical results for the new disentropy and q-diode are provided.

© 2020 Elsevier B.V. All rights reserved.

1. Introduction

The Lambert W function is an important multivalued function that finds applications in different areas of mathematics, computer Science and physics [1–6]. The Lambert W function is defined as the solution of the equation

$$W(z)\, e^{W(z)} = z. \tag{1}$$

In the interval $-1/e \leq x \leq 0$ there exist two real values of $W(z)$. The branch for which $W(x) \geq -1$ is the principal branch named $W_0(z)$ while the branch satisfying $W(z) \leq -1$ is named $W_{-1}(z)$. For $x \geq 0$ only $W_0(z)$ is real and for $x < -1/e$ there are not real solutions. The point $(z_b = -1/e, W(z_b) = -1)$ is the branch point where the solutions W_0 and W_{-1} have the same value.

On the other hand, the q-exponential function proposed by Tsallis [7] is given by

$$e_q{}^z = \begin{cases} e^z & q = 1 \\ [1 + (1-q)\, z]^{1/(1-q)} & q \neq 1 \cap 1 + (1-q)\, z \geq 0 \\ 0 & q \neq 1 \cap 1 + (1-q)\, z < 0 \end{cases} \tag{2}$$

Using Tsallis q-exponential (2) in the Lambert equation (1), one has the Lambert–Tsallis equation [8]

$$W_q(z)\, e_q{}^{W_q(z)} = z \tag{3}$$

whose solutions are the Lambert–Tsallis W_q functions. Using the definition of $\exp_q$ given in Eq. (2) in Eq. (3), the W_q function can be found solving the equation [8]

$$x(r + x)_+{}^r = r^r z, \tag{4}$$

E-mail address: rubens.ramos@ufc.br.

https://doi.org/10.1016/j.physa.2020.124851
0378-4371/© 2020 Elsevier B.V. All rights reserved.

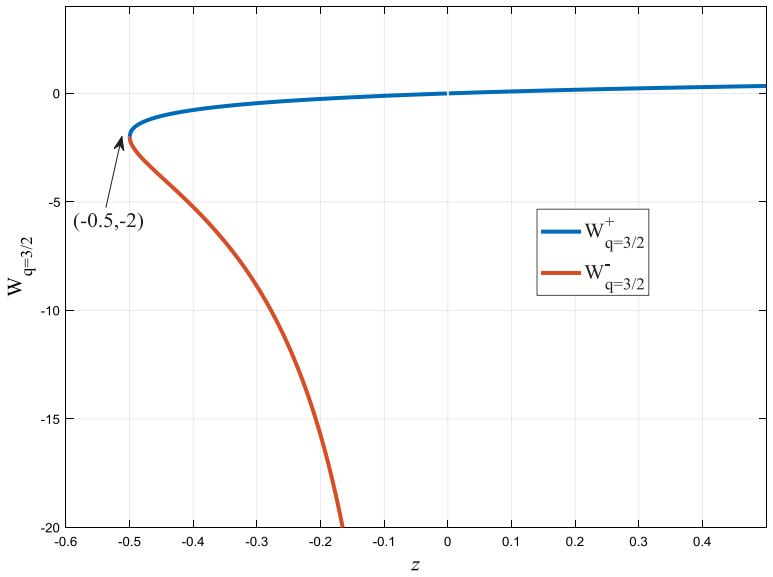

Fig. 1. $W_{q=3/2}$ versus z.

where $x = W_{\frac{(r-1)}{r}}(z)$, $r = 1/(1-q)$ and $(x)_+ = \max\{x,0\}$. When $q = 1$, one has $e_1(z) = e^z$ and, consequently, $W_1(z) = W(z)$. For example, for $q = \{2, 3, 3/2, 1/2\}$ one has the following Lambert–Tsallis W_q upper branches (upper index '+')

$$W_2(z) = \frac{z}{z+1}, \qquad z > -1, \tag{5}$$

$$W_3(z) = z\sqrt{z^2+1} - z^2 \qquad z \geq 0. \tag{6}$$

$$W^+_{3/2}(z) = \frac{2\,(z+1) + 2\sqrt{2z+1}}{z}, \qquad z > -1/2, \tag{7}$$

$$W^+_{1/2}(z) = \frac{\left[3\sqrt[3]{2z + \sqrt{\left(2z+\frac{8}{27}\right)^2 - \frac{64}{729}} + \frac{8}{27}} - 2\right]^2}{9\sqrt[3]{2z + \sqrt{\left(2z+\frac{8}{27}\right)^2 - \frac{64}{729}} + \frac{8}{27}}}, \qquad z \geq -0.29629, \tag{8}$$

Fig. 1 shows the plot of $W_{q=3/2}$ (upper '+' and lower '–' branches) versus z.
More details about the Lambert–Tsallis function and its applications can be found in [8–15].
In order to handle with the $\exp_q$ function, one has to use the q-operations. The important ones used in this work are:

$$a \times_q b = \max\left\{\left[a^{(1-q)} + b^{(1-q)} - 1\right]^{1/(1-q)}, 0\right\} \equiv \left[a^{(1-q)} + b^{(1-q)} - 1\right]_+^{1/(1-q)} \tag{9}$$

$$\left(e_q^x\right)^\alpha = e^{\alpha x}_{1-(1-q)/\alpha}. \tag{10}$$

2. The $R_{q,Q}$ function

In this section a new function is introduced. It is named $R_{q,Q}$ function and it is the solution of the following equation

$$R_{q,Q}(z) \times_Q e_q^{R_{q,Q}(z)} = z. \tag{11}$$

Eq. (11) is the Lambert–Tsallis equation using the q-product operation. Obviously, $R_{q,Q=1}(z) = W_q(z)$. Using (2) and (9) in (11) one gets

$$R^{1-Q}_{q,Q}(z) + \left[1 + (1-q)\,R_{q,Q}(z)\right]^{\frac{1-Q}{1-q}} - \left(z^{1-Q} + 1\right) = 0. \tag{12}$$

The general solutions of (12) will be published elsewhere. Here, the important case for introduction of a new disentropy and the q-diode modelling is $Q = q$. In this case Eq. (12) is reduced to

$$R^{1-q}_{q,q}(z) + (1-q)\,R_{q,q}(z) - z^{1-q} = 0. \tag{13}$$

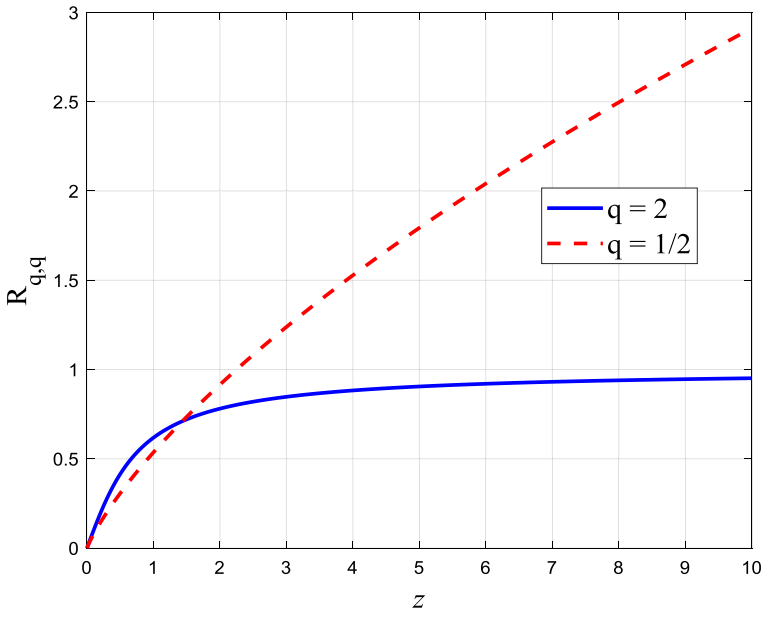

Fig. 2. $R_{q,q}(z)$ versus z for $q = 1/2$ and $q = 2$.

For example, for $q = 2$ and $q = 1/2$ one has

$$R_{2,2}(z) = -\frac{1}{2z} \pm \frac{1}{2z}\sqrt{1+4z^2}, \tag{14}$$

$$R_{1/2,1/2}(z) = 2\left(z^{1/2}+1\right) - 2\sqrt{2z^{1/2}+1}. \tag{15}$$

Fig. 2 shows the plot of the parts of the functions $R_{2,2}$ and $R_{1/2,1/2}$ that obey Eq. (11).

3. Disentropy

The disentropy based on the Lambert and Lambert–Tsallis functions and its applications in quantum and classical information theory, image processing and black hole, among others, have been discussed in [8–14]. Taking the $\log_q$ in both sides of Eq. (11) with $q = Q$, one gets

$$\log_q(z) = R_{q,q}(z) + \log_q\left[R_{q,q}(z)\right]. \tag{16}$$

Hence, Tsallis q-entropy can be written as

$$S_q = -\sum_i p_i^q \log_q(p_i) = -\sum_i p_i^q R_{q,q}(p_i) - \sum_i p_i^q \log_q\left[R_{q,q}(p_i)\right]. \tag{17}$$

The term

$$D_{q,q} = \sum_i p_i^q R_{q,q}(p_i) \tag{18}$$

is a disentropy. It can be shown it is maximal for delta distribution and minimal for a uniform distribution. Its quantum version is

$$D_{q,q}(\rho) = \sum_i \lambda_i^q R_{q,q}(\lambda_i) \tag{19}$$

where λ_i is the ith eigenvalue of the density matrix ρ. The disentropy based on the $R_{q,q}$ function can be used in the same problems that the disentropy based on the Lambert–Tsallis function is used. For example, it can be used to measure the disentanglement of bipartite of qubit states [8]. Fig. 3 shows the behaviour of $D_{q,q}$ for the distribution $\{p,1\text{-}p\}$ using the values $q = 0.5$, $q = 1$ and $q = 2$.

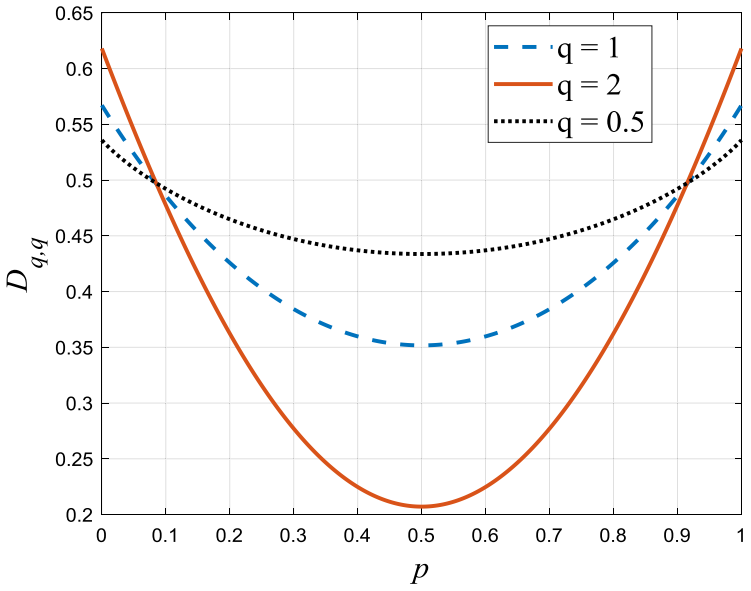

Fig. 3. Disentropy of the distribution {p, 1-p} versus p for $q \in [0.5, 1, 2]$.

In [10] the continuous disentropy (based on the Lambert–Tsallis $W_{q=2}$ function) of the Wigner function was used to measure the quantumness of a physical state,

$$D_q = \int_y \int_x w^q (x, y)\, W_q (w (x, y))\, dxdy \Rightarrow D_2 = \int_y \int_x \frac{w^3 (x, y)}{1 + w (x, y)} dxdy, \tag{20}$$

where $w(x, y)$ is the Wigner function of the physical state considered. Although Eq. (20) can detect quantumness, it is not good for measuring entanglement or disentanglement since it can return a negative value. Aiming to overcome this problem, a new formula was proposed, the disentropy based on the Rényi entropy [13]:

$$D_{q,\alpha} = W_q \left(\iint_{x,y} w^\alpha (x, y)\, dxdy \right). \tag{21}$$

Although any value of q can be used in Eq. (21), only $\alpha = 2$ (or even numbers) is used. In this case the information contained in the signal of the Wigner function is lost. In order to have a disentanglement measure that takes into account the signal of the Wigner function, the following continuous disentropy is here proposed

$$D_{q,q} = \int_y \int_x w^q (x, y)\, R_{q,q} (w (x, y))\, dxdy \Rightarrow D_{2,2} = \int_y \int_x \frac{w (x, y)}{2} \left(\sqrt{1 + 4w^2 (x, y)} - 1 \right) dxdy. \tag{22}$$

One may note that $R_{2,2}$ is always positive. In order to test Eq. (22), the bipartite quantum state described in [16] is considered:

$$|\psi\rangle = \frac{(1 + ad)}{\sqrt{(1 + ad)^2 + a^2 d}} |00\rangle - \frac{1}{\sqrt{2}} \frac{a\sqrt{d}}{\sqrt{(1 + ad)^2 + a^2 d}} |02\rangle - \frac{1}{\sqrt{2}} \frac{a\sqrt{d}}{\sqrt{(1 + ad)^2 + a^2 d}} |20\rangle, \tag{23}$$

where a is an interpolation parameter and $D = 2d$ is the number of dimensions of the bipartite system. The eigenvalues of the partial trace of (23) are

$$\lambda_\pm = \frac{1}{2} \left\{ 1 \pm \left[1 - \left(\frac{a^2 d}{(1 + ad)^2 + a^2 d} \right)^2 \right]^{\frac{1}{2}} \right\}. \tag{24}$$

Thus, the disentanglement of the bipartite state (23) is

$$D_{q,q} (\psi) = \lambda_+^q R_{q,q} (\lambda_+) + \lambda_-^q R_{q,q} (\lambda_-). \tag{25}$$

On the other hand, the Wigner function of the state (23) is

$$w (r, k) = \pi^{-D} e^{-r^2 - k^2} \left[1 + a \left(\gamma_- r^2 - \gamma_+ k^2 + \gamma \left(r^2 + k^2 \right) - 4\gamma r^2 k^2 \sin^2 (\theta) \right) \right] \tag{26}$$

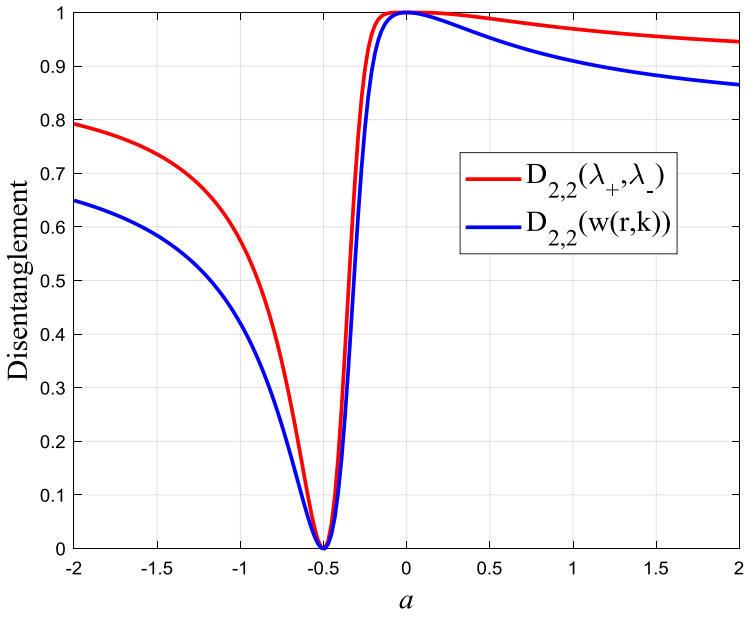

Fig. 4. Disentanglement of the state (23) using $D_{2,2}(\lambda_+, \lambda_-)$ (Eq. (25)) and $D_{2,2}(w(r, k))$ (Eq. (22)) versus a, for $D = 4$ and $\theta = 5\pi/12$. Both disentropies were normalized.

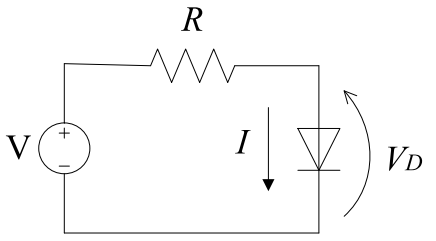

Fig. 5. Electrical circuit with a resistor and a diode.

where

$$\gamma_{\pm} = 2\frac{1 + aD/2 \pm a}{(1 + aD/2)^2 + a^2D/2} \tag{27}$$

$$\gamma = \frac{a}{(1 + aD/2)^2 + a^2D/2}. \tag{28}$$

The bipartite disentanglement of the state (23) versus a measured by Eqs. (25) and (22) and (26)–(28), for $D = 4$ and $\theta = 5\pi/12$, can be seen in Fig. 4.

As expected, the minimal disentanglement (maximal entangled state) occurs in $a = -2/D = -0.5$ and the maximal disentanglement (separable state) occurs in $a = 0$.

4. The q-diode

For a semiconductor diode that obeys the simplified Shockley's model, the relation between current and voltage is given by

$$I = I_s e^{\frac{V_D}{\eta V_T}}, \tag{29}$$

where I_s is the saturation current of the diode, V_D is the voltage between the diode terminals, $V_T = kT/q_e$ ($q_e -$ electron charge, $k -$ Boltzman constant, $T -$ temperature) and, finally, η is the diode ideality factor ($1 < \eta < 2$ for silicon diodes). Fig. 5 shows the very basic electrical circuit composed by a power supply, a resistor and the diode.

The current that flows through the diode in the circuit shown in Fig. 5 is given by

$$I = I_s e^{\frac{V - RI}{\eta V_T}}. \tag{30}$$

Using the Lambert W function in (30) one gets the following relation between electrical current (I) and power supply voltage (V)

$$I = \frac{\eta V_T}{R} W\left(\frac{I_s R}{\eta V_T} e^{\frac{V}{\eta V_T}}\right). \tag{31}$$

More details about the applications of the Lambert function in the analytical solution of some electronic circuits can be found in [17–20].

The q-diode, by its turn, is defined as the hypothetical device whose relation between current and voltage between its terminals (V_D) is given by

$$I = I_s e_q^{\frac{V_D}{\eta V_T}}. \tag{32}$$

Using the q-diode in the circuit shown in Fig. 5, the value of the electric current flowing through the diode is given by

$$I = I_s e_q^{\frac{V-IR}{\eta V_T}}. \tag{33}$$

Using the q-operations in (33) one gets

$$I = I_s e_q^{\frac{V-IR}{\eta V_T}} \Rightarrow \frac{IR/\eta V_T}{I_s R/\eta V_T} = e_q^{\frac{V}{\eta V_T}} \div_q e_q^{\frac{IR}{\eta V_T}} \Rightarrow \frac{IR/\eta V_T}{I_s R/\eta V_T} \times_q e_q^{\frac{IR}{\eta V_T}} = e_q^{\frac{V}{\eta V_T}}. \tag{34}$$

Now, using the function $R_{q,q}$ in (34), after some algebra one gets the following solutions for the electrical current I, for $q = 2$ and $q = 0.5$,

$$I_2(V) = \frac{\eta V_T}{R}\left[-\frac{1}{2e_q^{\frac{V}{\eta V_T}}} + \frac{1}{2}\sqrt{\left(e_q^{\frac{V}{\eta V_T}}\right)^{-2} + \frac{4\eta V_T}{I_s R}}\right], \tag{35}$$

$$I_{1/2}(V) = \frac{\eta V_T}{R}\left[2\left(\left(e_q^{\frac{V}{\eta V_T}}\right)^{1/2} + \frac{\eta V_T}{I_s R}\right) - 2\sqrt{2\frac{\eta V_T}{I_s R}\left(e_q^{\frac{V}{\eta V_T}}\right)^{1/2} + \left(\frac{\eta V_T}{I_s R}\right)^2}\right]. \tag{36}$$

One may note that (35) and (36) are, respectively, equal to (14) and (15) when $(\eta V_T/I_s R) = 1$. The q-diode that follows the non-simplified Shockley's model has the following current $\times$ voltage relation

$$I = I_s\left(e_q^{\frac{V_D}{\eta V_T}} - 1\right). \tag{37}$$

Using Eq. (37) in the circuit shown in Fig. 5, one gets for the electric current the equation

$$I = I_s\left(e_q^{\frac{V-RI}{\eta V_T}} - 1\right). \tag{38}$$

After some algebra one easily gets

$$\frac{I_s R\,(i+1)/\eta V_T}{I_s R/\eta V_T} \times_q e_q^{\frac{I_s R(i+1)}{\eta V_T}} = e_q^{\frac{V+I_s R}{\eta V_T}}, \tag{39}$$

where $i = I/I_s$. The solutions for $q = 2$ and $q = 1/2$ are, respectively,

$$I_2(V) = \frac{\eta V_T}{I_s R}\left[-\frac{1}{2e_q^{\frac{V+I_s R}{\eta V_T}}} + \frac{1}{2}\sqrt{\left(e_q^{\frac{V+I_s R}{\eta V_T}}\right)^{-2} + \frac{4\eta V_T}{I_s R}}\right] - 1, \tag{40}$$

$$I_{1/2}(z) = \frac{\eta V_T}{I_s R}\left[2\left(\left(e_q^{\frac{V+I_s R}{\eta V_T}}\right)^{1/2} + \frac{\eta V_T}{I_s R}\right) - 2\sqrt{2\frac{\eta V_T}{I_s R}\left(e_q^{\frac{V+I_s R}{\eta V_T}}\right)^{1/2} + \left(\frac{\eta V_T}{I_s R}\right)^2}\right] - 1. \tag{41}$$

In Fig. 6 one can see the solutions of Eq. (39) for the cases $q = 1$, $q = 0.75$ and $q = 1/2$. The smaller the value of q the slower is the growth of the current. The q-diode with $q > 1$ operates at very low voltage since $\exp_q(x)$ goes too fast to zero. For example, for $q = 1.25$, one must have $V/(\eta V_T) < 4$ ($V < \sim 0.1$ mV).

Compared to the classical diode, the q-diode with $q > 1$ has to operate with lower voltage while the q-diode with $q < 1$ requires a larger voltage. Since, the q-diode shows the nonlinear behaviour (between I and V) it can be used in telecommunications equipment working as a modulator or mixer, for example. Furthermore, like the ordinary diode, the current flowing through the q-diode depends on the bias applied (forward or reverse). Thus, the q-diode can also be used

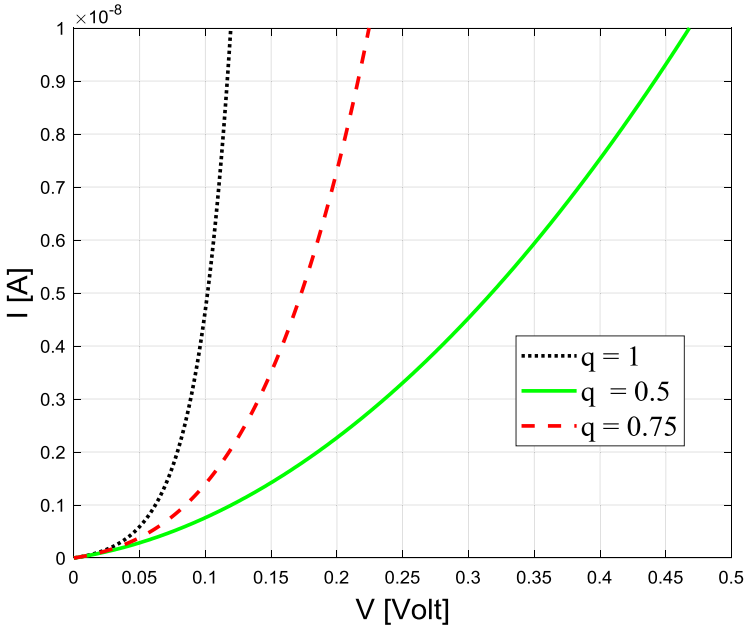

Fig. 6. q-Diode current versus voltage curve for $q \in [0.5, 0.75, 1]$.

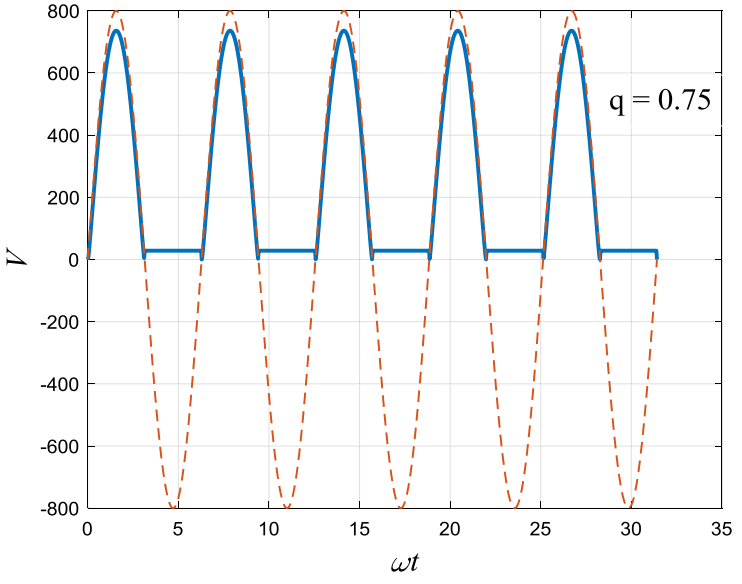

Fig. 7. Input and output of a half-wave rectifier using a q-Diode with $q = 0.75$. The input signal is $V_{in} = 800\ \sin(\omega t)$.

in power electronic circuits like half-wave and full-wave rectifier circuits, as well in clipping circuits. In Fig. 7 one can see the q-diode ($q = 0.75$) working correctly as half-wave rectifier. The input signal is $V_{in} = 800\ \sin(\omega t)$ (dashed line) and the output signal is V (solid line). The voltage between the q-diode terminals is ∼64V (one hundred times larger than the voltage between the terminals of a silicon diode).

In Fig. 8 the q-diode ($q = 0.75$) is also working in a half-wave rectifier circuit. However, the input signal is $V_{in} = 100\sin(\omega t)$ (dashed line). In this case, the input voltage is not large enough to make the q-diode to work in the correct operation point and, hence, the output signal, V (solid line), is not correctly rectified.

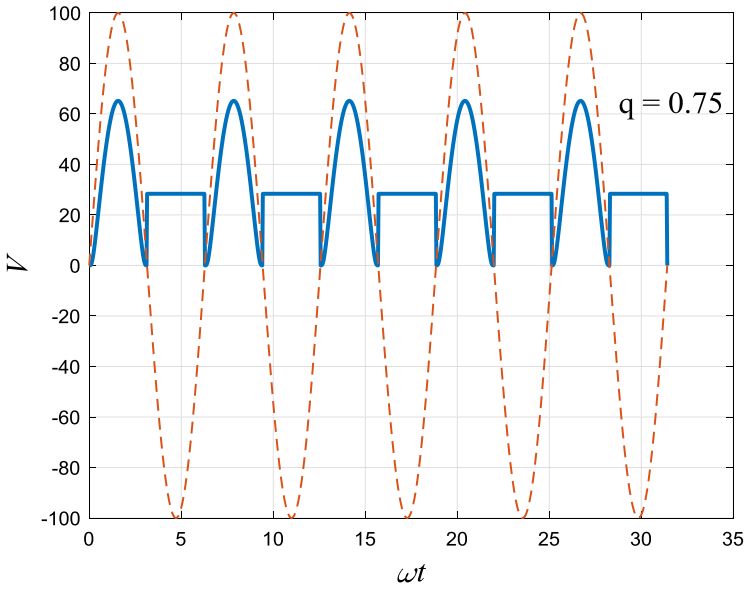

Fig. 8. Input and output of a half-wave rectifier using a q-Diode with $q = 0.75$. The input signal is $V_{in} = 100\ \sin(\omega t)$. The output voltage is deformed because the q-diode is not working in the correct operation point.

5. Conclusions

Initially, the present work introduced the solutions of the equation $R_{q,\mathrm{Q}}(z) \times_{\mathrm{Q}} \exp_q(R_{q,\mathrm{Q}}(z)) = z$ and showed two applications of the function $R_{q,\mathrm{Q}}(z)$: (1) It was used to construct a new disentropy formula. This new disentropy can be applied in a large variety of problems in physics and engineering. A full comparison between the disentropy based on the $R_{q,q}$ function and the disentropy based on the Lambert–Tsallis W_q function is a question for future investigation. (2) The $R_{q,q}$ function was used to model the q-diode. Basically, different values of q results in q-diodes operating in different voltages. q-Diodes with $q > 1$ ($q < 1$) are devices that work with small (large) signals. Which values of q will result in a q-diode that can be physically realized is still a problem to be investigated.

CRediT authorship contribution statement

R.V. Ramos: Conceptualization, Methodology, Software, Data curation, Writing - original draft, Visualization, Investigation, Validation, Writing - review & editing.

Declaration of competing interest

The authors declare that they have no known competing financial interests or personal relationships that could have appeared to influence the work reported in this paper.

Acknowledgements

This study was financed in part by the Coordenação de Aperfeiçoamento de Pessoal de Nível Superior I– Brasil (CAPES) – Finance Code 001, and CNPq, Brazil via Grant no. 307184/2018-8. Also, this work was performed as part of the Brazilian National Institute of Science and Technology for Quantum Information.

References

[1] R.M. Corless, G.H. Gonnet, D.E.G. Hare, D.J. Jeffrey, D.E. Knuth, On the Lambert W function, Adv. Comput. Math. 5 (1996) 329–359.
[2] S.R. Valluri, D.J. Jeffrey, R.M. Corless, Some applications of the Lambert W function to physics, Can. J. Phys. 78 (9) (2000) 823–831.
[3] D.C. Jenn, Applications of the Lambert W function in electromagnetics, IEEE Antennas Propag. Mag. 44 (3) (2002).
[4] F.C.- Blondeau, A. Monir, Numerical evaluation of the Lambert W function and application to generation of generalized Gaussian noise with exponent $\frac{1}{2}$, IEEE Trans. Signal Process. 50 (9) (2002) 2160–2165.
[5] D. Veberic, Having fun with Lambert $W(x)$ function, GAP-2009-114 [Online]. Available: http://arxiv.org/abs/1003.1628.
[6] K. Roberts, S.R. Valluri, Tutorial: The quantum finite square well and the Lambert W function, Can. J. Phys. 95 (2) (2017) 105–110.
[7] C. Tsallis, Possible generalization of Boltzmann–Gibbs statistics, J. Stat. Phys. 52 (1988) 479.
[8] G.B. da Silva, R.V. Ramos, The Lambert-Tsallis W_q function, Physica A 525 (2019) 164–170, http://dx.doi.org/10.1016/j.physa.2019.03.046.

[9] L.E. da Silva, G.B. da Silva. R. V. Ramos, The lamber-kaniadakis W_κ function, Phys. Lett. A (2019) http://dx.doi.org/10.1016/j.physleta.2019.126175.
[10] R.V. Ramos, Disentropy of the Wigner function, J. Opt. Soc. Am. B 36 (8) (2019) 2244–2249.
[11] J.L.M. da Silva, F.V. Mendes, R.V. Ramos, Radial basis function network using Lambert–Tsallis W_q function, Physica A 534 (2019) 122168, 1-9.
[12] R.V. Ramos, Quantum and classical information theory with disentropy, 2020, ArXiv/quant-ph:1901.04331.
[13] J.L.E. da Silva, R.V. Ramos, Calculation of the disentropy of the Wigner function using the Lambert-Tsallis W_q function with non-integer q values, J. Opt. Soc. Am. B 37 (7) (2020) 2035–2040.
[14] L.E. da Silva, G.B. da Silva, R.V. Ramos, Applications of Lambert-Tsallis and Lambert-Kaniadakis functions in differential and difference equations with deformed exponential decay, 2020, arXiV/cond-mat:2001.11995.
[15] R.V. Ramos, Using the Lambert-Tsallis function in the solution of basic relativistic problems, 2020, Researchgate.net.
[16] J.P. Dahl, H. Mack, A. Wolf, W.P. Schleich, Entanglement versus negative domains of Wigner functions, Phys. Rev. A 74 (2006) 042323, 1-7.
[17] T.C. Banwell, A. Jayakumar, Exact analytical solution for current flow through diode with series resistance, Electron. Lett. 36 (2000) 291–292.
[18] Adelmo Ortiz-Conde, Francisco J. Garcıá Sánchez, Juan Muci, Exact analytical solutions of the forward non-ideal diode equation with series and shunt parasitic resistances, Solid-State Electron. 44 (10) (2000) 1861–1864.
[19] Denise Lugo-Muñoz, Juan Muci, Adelmo Ortiz-Conde, Francisco J. García-Sánchez, Michelly de Souza, Marcelo A. Pavanello, An explicit multi-exponential model for semiconductor junctions with series and shunt resistances, Microelectron. Reliab. 51 (12) (2011) 2044–2048.
[20] A. Bernardini, K.J. Werner, A. Sarti, J.O. Smith, Modeling nonlinear wave digital elements using the Lambert function, IEEE Trans. Circuits Syst. I. Regul. Pap. 63 (8) (2016) 1231–1242.